

# Effect of substrate on growth of $WS_2$ thin films

M. Genut, L. Margulis, R. Tenne and G. Hodes

Department of Materials and Interfaces, Weizmann Institute of Science, Rehovot 76100 (Israel)

(Received February 25, 1992; accepted May 13, 1992)

## Abstract

Thin sputtered tungsten films on various substrates (molybdenum or tungsten foils, quartz and glass slides) were reacted with  $H_2S$  at temperatures from 400 to 1000 °C. In general, it was found that the  $WS_2$  crystallites nucleate from an amorphous  $WS_3$  phase. It was established that the substrate has a critical role in determining both the reaction onset temperature and the texture. For glass substrates, the reaction to give  $WS_2$  begins at  $T \geq 400$  °C, and the  $WS_2$  grains grow predominantly with the van der Waals (vdW) planes parallel to the substrate (in this orientation, the  $c$  axis is perpendicular to the substrate, and is designated  $\perp c$ ) at 500 °C. On quartz substrates, reaction begins only at 650 °C and the texture is predominantly vdW planes perpendicular to the substrate (this orientation is designated  $\parallel c$ ) below 950 °C, and exclusively  $\perp c$  texture at higher temperatures. These differences between glass and quartz are believed to be due to sites on the quartz, absent (or present to a smaller extent) on glass, which strongly bind the tungsten and  $WS_2$ . Molybdenum substrates give only the  $\parallel c$  orientation even at 1000 °C, while bulk tungsten (or tungsten sputtered on tungsten) gives randomly oriented  $WS_2$ . For oxidized tungsten on quartz, reaction onset is lowered to 500 °C (compared with 650 °C for W/quartz), and predominantly  $\perp c$  orientation is obtained at 800 °C. Exclusively  $\perp c$  orientation was never achieved with this system, even at 1000 °C. It was found that the  $\parallel c$  orientation changes to the  $\perp c$  orientation when diffusion conditions (temperature and time) were sufficient, indicating that the latter orientation is energetically favourable.

## 1. Introduction

Layered-structure transition metal dichalcogenides,  $MX_2$  ( $M \equiv W, Mo$ ;  $X \equiv S, Se$ ) have been investigated largely for their photovoltaic [1, 2] and lubricating [3] properties. The layered structure imparts a strong anisotropy of both mechanical and electrical properties.

Thin films of these compounds have been studied with respect to both tribological [3–6] and photovoltaic [7–9] properties. In both cases, films with van der Waals (vdW) planes parallel to the substrate ( $\perp c$  or type II films), rather than with the vdW planes perpendicular to the substrate ( $\parallel c$  or type I films), are desired, in particular for photovoltaic purposes; the  $\parallel c$  face of these materials normally exhibits very poor photovoltaic activity, and even a very small percentage of  $\parallel c$  orientation in a predominantly  $\perp c$  structure can severely degrade photovoltaic performance. These non-vdW plane defects act as recombination sites and centres for electrochemical corrosion [10].

Thin films of these materials have been grown principally by sputter deposition (mainly considered for their tribological properties) [4, 11, 12], and recently by selenization of tungsten or molybdenum films in a sealed tube [9]. Studies were carried out on the effects of preparation parameters on the texture ( $\parallel c$  or  $\perp c$ ) of

the films. For sputter-deposited films, water or hydroxide groups were found to promote  $\parallel c$  growth, either through contamination during growth [11] or as active sites on the substrate [12]. The latter was able to explain the effect of certain substrates on the film texture. By essentially removing  $H_2O$  or OH groups, predominantly  $\perp c$ -oriented films were obtained. Exclusively  $\perp c$ -oriented films were apparently never obtained, either by sputter deposition or by closed-tube selenization of tungsten or molybdenum films. Moser *et al.* [13] found that the first 5 nm of sputter-deposited  $MoS_2$  was  $\perp c$  oriented, but  $\parallel c$  growth occurred on this thin layer for thicker films.

In a previous paper [14] we reported on the microstructure of  $WS_2$  thin films grown by sulphiding thin sputtered tungsten films on quartz substrates, with emphasis on controlling the orientation of the  $WS_2$  crystallites. The onset of the reaction between tungsten and  $H_2S$  to give  $WS_2$  thin films was found to be 650 °C. Orientation of the  $WS_2$  crystallites could be controlled by choice of reaction temperature and sulphur concentration in the gas flow: low reaction temperatures and high sulphur concentrations lead to  $\parallel c$  growth, while high temperatures (1000 °C) and low sulphur concentrations result in  $\perp c$  growth, which is, as explained above, the desirable orientation. These results were

explained on the basis of a competition between the reaction rate to form the compound and the rate of crystallization. It was also found that, in order to obtain 100%  $\perp c$  orientation, the tungsten film must be sputtered at a moderate–high rate, possibly because of incorporation of contaminants in the growing film at low sputtering rates.

In the present work we used the same preparation procedures as before [14] to study the effect of the substrate on the texture and onset reaction temperatures. The results are compared for different substrates: molybdenum or tungsten foils, quartz and glass slides as well as bulk tungsten foils. We also studied the difference between oxidized and unoxidized tungsten films.

## 2. Experimental details

Thin films of tungsten (about 50 nm thick) were ion beam sputtered onto molybdenum or tungsten foils, quartz and glass slides. Before sputtering, the substrates were carefully degreased in an ultrasonic bath with trichloroethylene and ethanol. The background pressure in the chamber was no more than  $2 \times 10^{-6}$  mbar ( $2 \times 10^{-4}$  Pa) and sputtering was carried out with an argon pressure (in the chamber) of  $2 \times 10^{-4}$  mbar ( $2 \times 10^{-2}$  Pa). Before the metal sputtering, the substrate was sputter etched for a few minutes until the pressure in the chamber was stabilized. The sputtering rate of tungsten was about  $10 \text{ nm min}^{-1}$ . Tungsten foils without any deposition were also used for comparison with thin films. Part of the specimen of each set (W/Mo, W/W, W, W/quartz and W/glass) was oxidized in air at  $500^\circ\text{C}$  for 1 h.

The samples were then reacted in a quartz furnace with a flow of  $H_2S$  ( $5\text{--}50 \text{ ml min}^{-1}$ ) and forming gas ( $5\% H_2, 95\% N_2, 150 \text{ ml min}^{-1}$ ). The reaction temperatures were controlled in the range from  $400$  to  $1000^\circ\text{C}$ . After the furnace reached the desired temperature and a uniform gas flow was maintained, the samples were introduced into the hot zone of the reaction chamber (by a magnet from outside the quartz tube) for periods from 5 min to several hours. After reaction the samples were moved back to the cold zone of the reaction chamber where a temperature close to room temperature (about  $60^\circ\text{C}$ ) was maintained.

The reaction products were analysed by X-ray diffraction (XRD) ( $Cu K\alpha$  radiation), transmission electron microscopy (TEM), electron probe microanalysis (EPMA), Auger electron spectroscopy (AES), optical transmission spectroscopy (OTS) and four-point probe sheet resistivity measurements.

Thin foils for TEM observations were prepared by immersing the samples in very dilute HF (about 1%), after which they detached from the substrates.

## 3. Results and discussion

### 3.1. W/Glass

In order to find the onset temperature of the reaction, the samples were reacted at temperatures from  $400$  to  $550^\circ\text{C}$  (higher temperatures were avoided to prevent melting of the glass slides). No reaction was observed by XRD and OTS following reactive heat treatment at  $400^\circ\text{C}$  for 30 min. However, by TEM, early stages of the reaction between tungsten and sulphur were detected at this temperature. Figure 1 demonstrates that three regions were observed in specimens from this

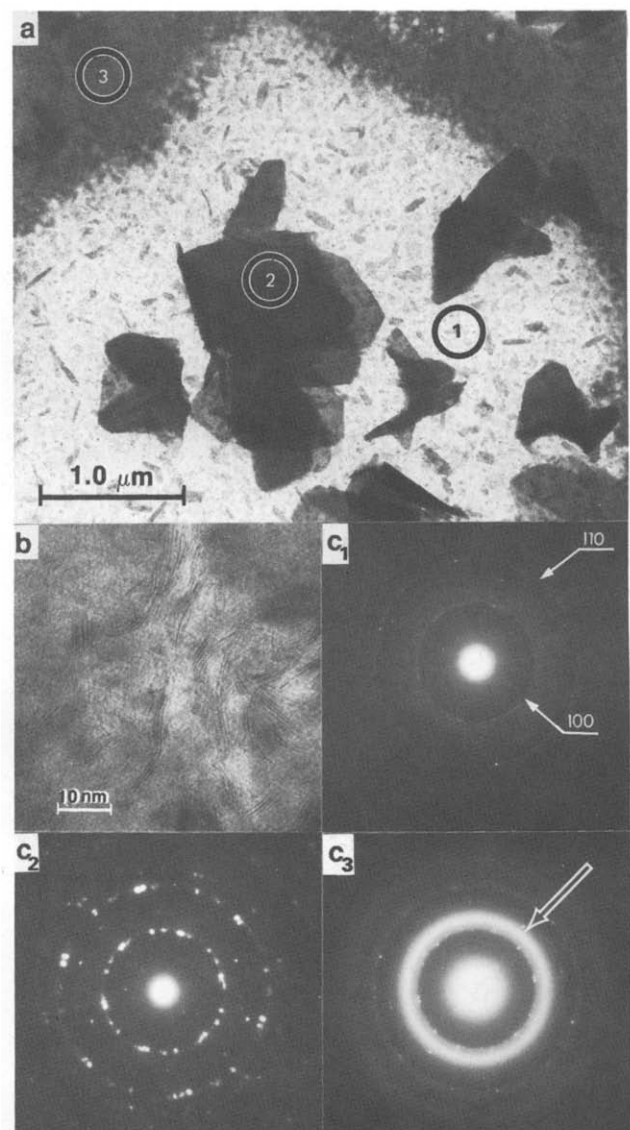


Fig. 1. TEM bright field (BF) images and selected area electron diffraction patterns (SADPs) from a film grown on a glass substrate at  $400^\circ\text{C}$  for 30 min. (a) General view showing three different areas: 1, thin layer; 2, large crystallites (overlapping); 3, thick layer. (b) Highly magnified region of the thin layer containing certain  $\parallel c$  grains. (c<sub>1</sub>), (c<sub>2</sub>), (c<sub>3</sub>) SADPs taken from areas 1, 2 and 3 respectively in (a).

initial stage: (1) thin layer; (2) large crystallites; (3) thick layer. The SADPs (Figs. 1(c<sub>1</sub>), 1(c<sub>2</sub>) and 1(c<sub>3</sub>)) were taken from areas 1, 2 and 3 respectively. From Fig. 1(c<sub>1</sub>) it can be seen that the thin region consists of the  $WS_2$  phase with  $\perp c$  texture. All the large crystallites have a clear  $\perp c$  orientation (Fig. 1(c<sub>2</sub>)). In addition, very small (10–30 nm) elongated crystallites with  $\parallel c$  orientation can also be observed at much higher magnification (Fig. 1(b)). Measurements of the diffraction patterns obtained from this early stage, as in Fig. 1, indicate a 5% increase in the lattice parameters of  $WS_2$  ( $a = 3.32 \text{ \AA}$ ,  $c$  could not be measured from this zone axis) compared with literature values and those found by us for all the  $WS_2$  specimens grown at higher temperatures. This may indicate a slight deviation in the stoichiometry of the  $WS_2$  crystallites in the initial stages of their formation. Such an interpretation is supported by previous work where it was reported that the decomposition products of  $MoS_3$ , (see below) contain a large number of metal vacancies giving rise to a deviation from the stoichiometric composition  $MoS_2$  [15]. In the SADP taken from the thick region we observe, in addition to the phases mentioned above, the appearance of an extra diffraction ring which corresponds to an amorphous phase with  $d = 2.41 \text{ \AA}$  (Fig. 1(c<sub>3</sub>), arrowed). This ring cannot be ascribed to tungsten, sulphur or  $WS_2$ . It does correspond, however, to the preferential W–S bond length (2.41  $\text{\AA}$ ) measured for amorphous  $WS_3$  [16]. Amorphous  $WS_3$  has been reported to be metastable [15, 17]; it subsequently transforms to the more stable phases  $WS_2$  and sulphur. It is also reasonable to ascribe this diffraction ring to  $WS_3$  since the reaction occurs with a significant excess of sulphur compared with tungsten,

and indeed the XRD spectra taken from specimens reacted at 450 °C exhibit, in addition to the  $WS_2$  peaks, some extra peaks that can be indexed as sulphur (*Powder Diffraction File* (PDF), Card 8-247). We recall that, in our study of  $WS_2$  growth on quartz substrates [14], the amorphous phase was also detected at very early stages of  $WS_2$  formation even at 1000 °C. We conclude that the  $WS_2$  crystallites nucleate from the initially formed amorphous  $WS_3$  phase. BF and dark field (DF) magnified micrographs taken from the thin layer described in Fig. 1 can be seen in Fig. 2. The DF image taken from one of the  $WS_2$  {100} reflections clearly demonstrates that it consists of nanocrystallites with  $\perp c$  texture, although about 1% of  $\parallel c$  nanocrystallites also exist in this region as seen in Fig. 1(b).

The onset of the reaction can be observed by XRD and OTS only at temperatures of 450 °C or more. The reaction to give  $WS_2$  was completed at 500 °C (30 min). The stoichiometry was verified by EPMA. AES depth profiles indicated uniform tungsten and sulphur signals. No contamination was seen within the sensitivity of the experimental method (about 0.2 at.%). Previously [14], a significantly higher onset temperature (650 °C) was found for the quartz substrates.

In order to see whether this difference in onset temperature was due to differences in the tungsten film on the two substrates, a TEM study of tungsten removed from glass and from quartz was made. In both cases, electron diffraction revealed a rather wide diffuse ring corresponding to the {110} reflection ( $d = 2.238 \text{ \AA}$ ). DF imaging showed the crystallite size to be *ca.* 1 nm. For W/glass, additional scattered crystallites of size *ca.* 5 nm were also observed.

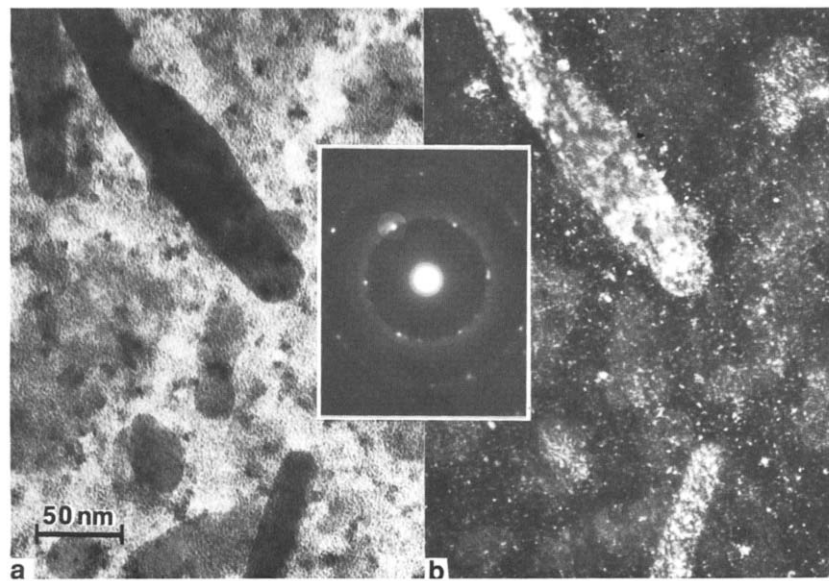


Fig. 2. TEM (a) BF image and (b) DF image taken from the thin layer described in Fig. 1. The inserted SADP shows the reflection that the DF image was taken from.

The surface morphology of the W/quartz film was smooth while the W/glass films were appreciably rougher. Since surface reaction usually occurs at a considerably lower temperature than bulk reaction, more of the W/glass film, with a higher real surface area, will react as surface than will the W/quartz film. However, unless the W/glass film is microporous (we do not see obvious evidence for this in the TEM pictures), this would not be expected to affect the bulk reactivity, although it should be remembered that the 50 nm thick tungsten film may not necessarily be considered to be bulk.

A further observed difference between the two tungsten films is that the adhesion of tungsten to quartz is considerably stronger than to glass. This suggests strong bonding, probably through oxygen links between the tungsten and quartz, which is absent, or much less frequent, for tungsten on glass. Unless sulphidation begins at the W-substrate interface, as could occur for a microporous film, this would not be expected to affect the reaction temperature.

A possible (although not measured) difference between the two tungsten films might be migration of atoms, such as alkali metals, from the glass into the thin tungsten film. Such an effect would not occur with quartz. Impurities in the tungsten film could affect many properties, including chemical reactivity, *e.g.* by inducing nucleation at a lower temperature.

A typical XRD spectrum from a specimen after 30 min of reaction at 500 °C is shown in Fig. 3. The main problem is to differentiate between the two existing polytypes: tungsten disulphide 2H hexagonal phase (PDF, Card 8-237) and the rhombohedral tungsten disulphide 3R phase (PDF, Card 35-651). Both phases have very close lattice parameters, making identification by XRD difficult. However, the 2H phase fits the data more accurately. Only the (001)-type reflections ( $l = 2n$ )

can be observed, indicating predominantly  $\perp c$  growth. We recall that, when quartz was used as a substrate, the nucleation was with  $\parallel c$  texture, and it changed to  $\perp c$  only at temperatures higher than 950 °C.

To explain the difference between the texture of the  $WS_2$  films on glass and quartz, the most likely, although less than completely convincing, property which controls this difference is the difference in adhesion of the tungsten films to the two substrates. Using the argument of Bertrand [12] together with the argument we discussed for the better adhesion of tungsten to quartz, we may expect that the oxygen-containing active sites, which bind the tungsten so firmly to quartz, force the growing  $WS_2$  to align with the dangling (more reactive) bonds toward the substrate, *i.e.*  $\parallel c$  growth. For glass, which does not possess such active sites (poor adhesion of tungsten), the vdW plane, which is the lowest energy surface, will lie parallel to the substrate in order to minimize the interfacial energy. As suggested by Bertrand [12], an amorphous substrate may also cause such  $\perp c$  alignment, which is satisfied by glass in this case.

We recognize a difference between Bertrand's model for sputtered films and for our films, which are formed from a pre-deposited tungsten film. In addition, while Bertrand finds  $\parallel c$  growth for  $WS_2$  deposited at room temperature, and predominantly  $\perp c$  growth for heated (220 °C) quartz, where  $H_2O$  or OH groups are eliminated, we find  $\parallel c$  growth for temperatures well above this. However, the strong adhesion of tungsten to quartz suggests that the active sites in our case are not merely adsorbed  $H_2O$  or  $-OH$  groups but part of the  $SiO_2$  lattice, which will not be removed on heating. Much higher temperatures (1000 °C) are apparently required to obtain the thermodynamically preferred, but kinetically unfavourable,  $\perp c$  growth.

Relatively large hexagonally shaped grains (about 0.25  $\mu m$ ) can clearly be observed in a typical film grown at 500 °C for 30 min (Fig. 4(a)). The SADP demonstrates that these grains have  $\perp c$  orientation (Fig. 4(b)). The fact that the reflections appear in pairs indicates the existence of two mutually rotated grains (one on top on the other). The diffraction pattern taken from the whole field of view (Fig. 4(c)) demonstrates that indeed the  $\perp c$  texture is predominant. However, the appearance of the innermost diffraction ring belonging to the {002} reflection indicates that some  $\parallel c$ -oriented grains also exist in this temperature regime. (Faint point reflections on the innermost diffraction ring seen in Fig. 4(b) did not correspond to  $\parallel c$  grains, and are most probably due to double diffraction.) Indeed, a magnified image of the circled area (inserted in Fig. 4(a)) reveals the presence of  $\parallel c$ -oriented grains. Exclusively  $\perp c$  growth was obtained only for the quartz substrates at much higher temperatures (1000 °C) [14] where the glass could not be used.

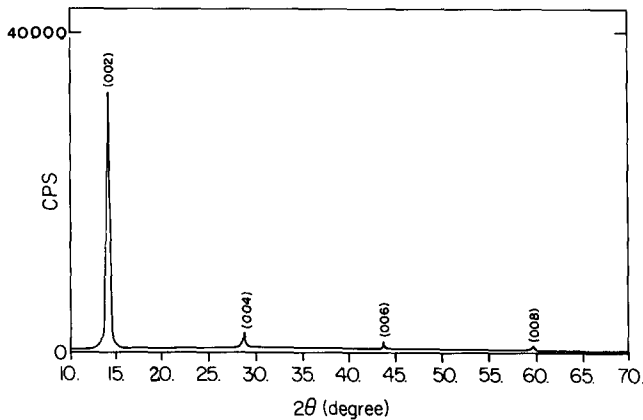


Fig. 3. Typical XRD spectrum from films grown on a glass substrate at 500 °C for 30 min, showing  $\perp c$  orientation.

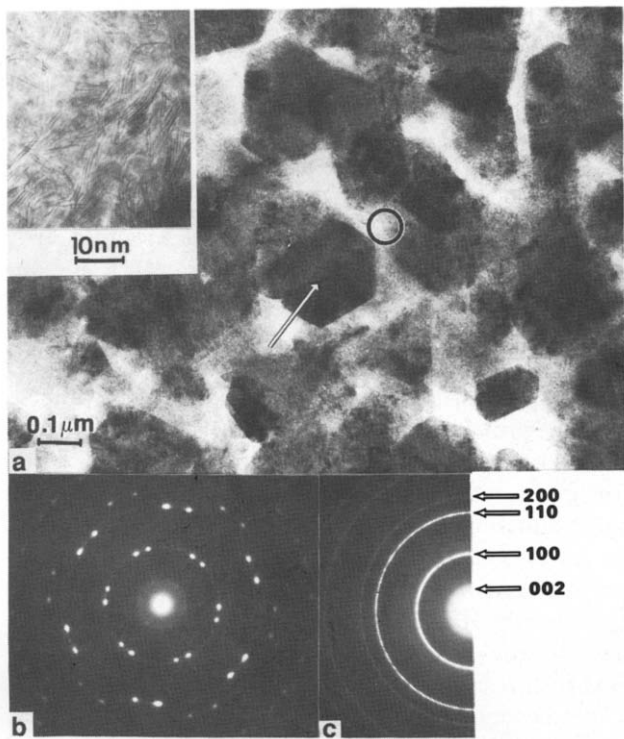


Fig. 4. TEM BF images of a film grown on a glass substrate at 500 °C for 30 min. (a) BF image (magnified image of the circled area, showing  $\parallel c$  grains, is inserted). (b) SADP from the arrowed hexagonal shaped grain in (a). (c) Indexed diffraction pattern from the whole field of view.

The results of the sheet resistivity measurements (four-point probe method) *vs.* reaction temperature (30 min of reaction) are given in Table 1. One can clearly see that the sheet resistivity is very sensitive to the onset of reaction temperature: the resistivity increases by 4 orders of magnitude between 450 °C and 500 °C, indicating transformation to semiconducting  $WS_2$ .

### 3.2. $WO_3/Quartz$

Specimens were prepared by oxidizing the W/quartz specimens in air at 500 °C for 1 h. By XRD and TEM it was found that the transparent yellowish layer obtained consisted of randomly oriented grains (about 250 nm) belonging to various  $WO_3$  phases. The specimens were subsequently reacted with  $H_2S$  at tempera-

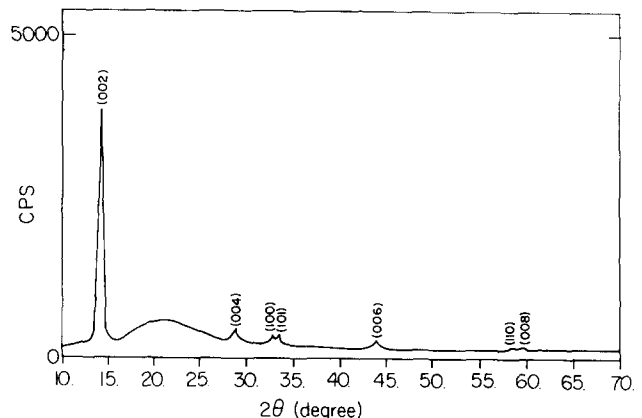


Fig. 5. Typical XRD spectrum from oxidized tungsten films on a quartz substrate, after growth at 1000 °C for 5 h, showing the predominantly  $\perp c$  texture.

tures between 400 and 1000 °C for times between 0.5 and 5 h.

We note two main differences between the results for the oxidized tungsten and those of the unoxidized tungsten reported by us in ref. 14.

(1) Using oxidized tungsten lowered the onset reaction temperature to 500 °C compared with 650 °C for the unoxidized case. The orientation was found by XRD and TEM to be  $\parallel c$  and it changed to predominantly  $\perp c$  texture after reaction at 800 °C.

(2) In the oxidized case, in contrast to the unoxidized case, 100%  $\perp c$  orientation was never obtained.

AES depth profiles reveal no significant difference between the  $WS_2$  formed from  $WO_3$  or tungsten. The oxygen concentration was below the detection limit in both cases.

A typical XRD spectrum taken from a specimen after reaction at 1000 °C for 5 h is shown in Fig. 5. Also here, similarly to the W/glass and W/quartz cases, XRD reveals that the  $\perp c$  texture is preferred. The intensity is *ca.* 10% of the XRD intensity found in Fig. 2 for glass substrates, indicating poorer crystallinity in this case. In addition, some low intensity XRD peaks belonging to {100}, {101} and {110} planes at  $2\theta = 32.767^\circ$ ,  $2\theta = 33.575^\circ$  and  $2\theta = 58.427^\circ$  respectively could also be observed, indicating that, with this system, one cannot obtain exclusively the  $\perp c$  orientation. This is supported by Buck [11] and Bertrand [12] who suggested that oxygen-containing species, such as  $H_2O$  and  $OH$ , adsorb on active sites that cause crystallites to grow with their basal planes perpendicular to the surface ( $\parallel c$  orientation). It is also important to note the fact that two diffraction peaks are obtained at  $2\theta \approx 33^\circ$ , rather than one with higher intensity, which would be expected for the 3R polytype. This supports our indexing the  $WS_2$  as the 2H polytype.

TABLE 1. Sheet resistivity as function of reaction temperature

Reaction temperature	$\rho$ ( $\Omega \text{ cm}$ )
As deposited	$5.5 \times 10^{-3}$
400 °C	$5.7 \times 10^{-3}$
450 °C	$2.5 \times 10^{-2}$
500 °C	120
550 °C	153

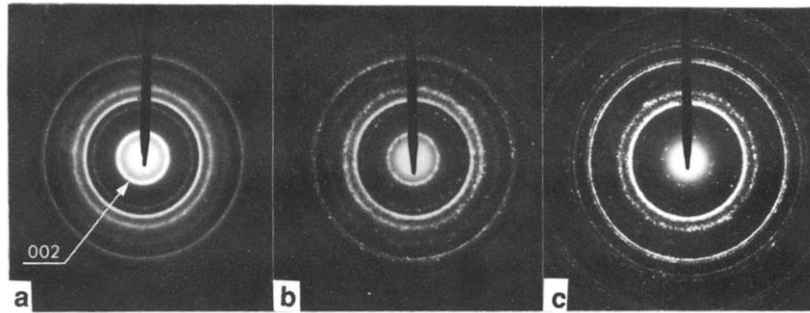


Fig. 6. SADPs taken from oxidized tungsten films on a quartz substrate, after growth at 1000 °C for (a) 1/2 h, (b) 2 h and (c) 3 h.

The TEM results are in agreement with the XRD data (Fig. 5). Predominantly  $\perp c$  grains were seen, in addition to some  $\parallel c$  nanocrystallites. This is similar to the growth shown in Fig. 4(a). Increases in the reaction temperature and time tend to increase the grain size and to decrease the number of  $\parallel c$ -oriented grains. The effect of decreasing  $\parallel c$  texture and changing to  $\perp c$  texture is demonstrated in Fig. 6, which shows electron diffraction patterns from specimens reacted at 1000 °C for 0.5, 2 and 3 h. It is clear that the first diffraction ring, the  $\{002\}$  reflection, decreases in intensity with increasing reaction time, indicating fewer  $\parallel c$ -oriented grains. This phenomenon actually indicates that, in contrast to what was previously believed [13, 14], in some cases  $\parallel c$ -oriented grains can reorder themselves to  $\perp c$  orientation at sufficiently high temperatures for long enough times. Therefore we conclude that the latter orientation is indeed energetically favourable as suggested previously by us [14]. This is in contrast to Moser *et al.* [13] who found that  $\perp c$  growth of  $MoS_2$  films can be turned into  $\parallel c$  but not the reverse. In recent experiments, highly textured  $MoS_2$  films with  $\perp c$  orientation were obtained [18], similar to the  $WS_2$  texture reported in this paper. These results show that the present sulphidation method is capable of producing the  $\perp c$  texture of layered compounds.

It is believed that the slow sulphidation described in this work allows the crystallites to orient themselves to the thermodynamically most favourable texture during growth, while sputtering of energetic species does not permit the relaxation of the texture during growth.

The sheet resistivity of these specimen was measured to be of the same order of magnitude as for the W/glass specimen (see Table 1), and 2 orders of magnitude higher than the W/quartz specimens reported in ref. 14.

### 3.3. $W/Mo$ , $WO_3/Mo$ , $W/W$ , and tungsten foils

In these systems, the reaction products were characterized mainly by XRD. A typical XRD spectrum of a W/Mo specimen after 15 min of reaction at 1000 °C is shown in Fig. 7. In addition to the molybdenum reflections, the main  $WS_2$  peaks are obtained at

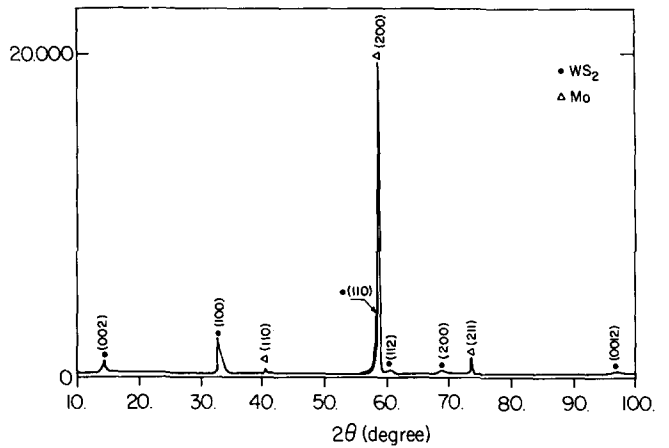


Fig. 7. Typical XRD spectrum from films grown on a molybdenum substrate at 1000 °C for 15 min, showing the predominantly  $\parallel c$  texture.

$d = 2.731 \text{ \AA}$  ( $2\theta = 32.767^\circ$ ) for the  $\{100\}$  reflection and at  $d = 1.578 \text{ \AA}$  ( $2\theta = 58.427^\circ$ ) for the  $\{110\}$  reflection. Since the most intense peak (100% intensity) according to the PDF, Card 8-237, should be at  $d = 6.18 \text{ \AA}$  ( $2\theta = 14.321^\circ$ ), we conclude that the  $WS_2$  grains grow with  $\parallel c$  texture. The  $\{002\}$  peak is relatively weak in spite of the theoretical (powder) intensity, indicating that only a minor fraction of the grains have  $\perp c$  orientation. We note that the location of the  $WS_2$   $\{110\}$  reflection with  $d = 1.578 \text{ \AA}$  ( $2\theta = 58.427^\circ$ ) is almost equal to the location of the molybdenum  $\{200\}$  peak with  $d = 1.574 \text{ \AA}$  ( $2\theta = 58.602^\circ$ ). In this case, partial epitaxy between the  $WS_2$  grains and the molybdenum substrate may be the reason for this orientation, even at 1000 °C, which is in contrast to our results [14] when quartz was used as a substrate and  $\perp c$  texture was usually obtained at reaction temperatures higher than 950 °C. (The molybdenum foils were found by XRD to have a  $\langle 100 \rangle$  texture, possibly because of the preparation by rolling.) Supporting our observations, the same  $\parallel c$  growth was reported by Mallouky and Bernede [19] when  $MoSe_2$  films were prepared by d.c. diode sputtering from an  $MoSe_2$  target onto molybdenum substrates.

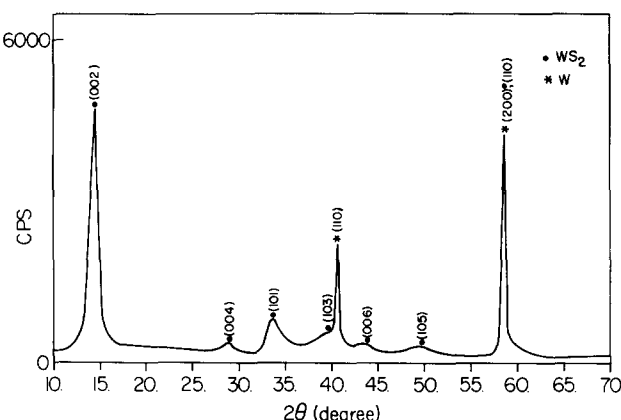


Fig. 8. Typical XRD spectrum from a tungsten foil (without any deposition), after reaction with  $H_2S$  at  $500\text{ }^\circ\text{C}$  for 1.5 h, showing no preferred texture.

The same XRD spectra (as in Fig. 7) were obtained when oxidized tungsten was used and then reacted with  $H_2S$  (the same conditions as above), which shows that here, also, the  $\parallel c$  texture is dominant.

Several tungsten foils without any deposition were reacted at  $500\text{ }^\circ\text{C}$  for up to 1.5 h. In this case, no preferred orientation was observed and the intensities correspond to PDF Card 8-237 (Fig. 8). The same results were obtained when a thin layer of tungsten was sputter deposited onto clean tungsten foils. When the reaction took place at temperatures of  $900\text{ }^\circ\text{C}$  and above, a black, very fine powder was very rapidly formed (in a few minutes), suggesting a very fast reaction between tungsten and  $H_2S$ . The XRD spectrum taken from this powder also corresponded to the PDF, Card 8-237, of  $WS_2$ . From these experiments, it is clear that thin  $WS_2$  films grow with a preferred orientation only when a thin tungsten layer is deposited on a suitable substrate. The thin tungsten film deposited on a tungsten substrate behaves as bulk tungsten to form randomly oriented  $WS_2$ .

#### 4. Conclusions

It is clear from the results obtained that the substrate has a critical role in determining both the temperature at which reaction between tungsten and  $H_2S$  occurs and the orientation of the final  $WS_2$  film. However, in general, the  $WS_2$  phase nucleates from the metastable  $WS_3$  amorphous phase.

For glass substrates, reaction occurs at  $400\text{ }^\circ\text{C}$ . The metastable amorphous  $WS_3$  phase is first formed and it decomposes with the formation of the stable  $WS_2$  phase. The  $WS_2$  film exhibits predominantly, although not exclusively,  $\perp c$  orientation at  $500\text{ }^\circ\text{C}$ .

For quartz substrates, reaction occurs at  $650\text{ }^\circ\text{C}$  and the orientation is predominantly  $\parallel c$  below  $950\text{ }^\circ\text{C}$ , and exclusively  $\perp c$  at higher temperatures. Molybdenum substrates give  $\parallel c$  orientation even at  $1000\text{ }^\circ\text{C}$  and bulk tungsten (or tungsten sputtered on tungsten) gives randomly oriented  $WS_2$ . It was suggested that the difference between glass and quartz substrates is due to stronger bonding of the tungsten and  $WS_2$  to quartz than to glass.

For oxidized tungsten ( $WO_3$ ) on quartz, the reaction onset is lowered to  $500\text{ }^\circ\text{C}$  (compared with  $650\text{ }^\circ\text{C}$  for W/quartz), and a predominantly  $\perp c$  orientation is obtained at  $800\text{ }^\circ\text{C}$ . However, an exclusively  $\perp c$  orientation was never achieved with this system, even at  $1000\text{ }^\circ\text{C}$ .

As expected, a rise in reaction temperature and prolongation of the reaction time (also post annealing) increase the grain size. Under these conditions, we found that  $\parallel c$ -oriented grains changed to  $\perp c$ , indicating that the latter orientation is energetically favourable.

#### Acknowledgments

This work was supported by a grant from the National Council for Research and Development, Israel, and the KFA, Jülich, FRG. L. M. thanks the Israel Ministry of Science for partial support.

#### References

- 1 W. Kautek, H. Gerischer and H. Tributsch, *J. Electrochem. Soc.*, **127** (1980) 2471.
- 2 R. Tenne and A. Wold, *Appl. Phys. Lett.*, **47** (1985) 707.
- 3 P. D. Fleischauer, *Thin Solid Films*, **154** (1987) 309.
- 4 R. Bichsel and F. Lévy, *Thin Solid Films*, **116** (1984) 367.
- 5 P. A. Bertrand, *J. Mater. Res.*, **4** (1989) 180.
- 6 H. Dimigen, H. Hübsch, P. Willich and K. Reichelt, *Thin Solid Films*, **64** (1979) 221.
- 7 G. Djemal, N. Müller, U. Lachish and D. Cahen, *Sol. Energy Mater.*, **5** (1981) 403.
- 8 H. D. Abruna and A. J. Bard, *J. Electrochem. Soc.*, **129** (1982) 673.
- 9 A. Jäger-Waldau and E. Bucher, *Thin Solid Films*, **200** (1991) 157.
- 10 A. Jäger-Waldau, M. Lux-Steiner, R. Jäger-Waldau, R. Burkhardt and E. Bucher, *Thin Solid Films*, **189** (1990) 339.
- 11 H. J. Lewerenz, A. Heller and F. J. DiSalvo, *J. Am. Chem. Soc.*, **102** (1980) 1877.
- 12 V. Buck, *Thin Solid Films*, **139** (1986) 157.
- 13 J. Moser, H. Liao and F. Lévy, *J. Phys. D.*, **23** (1990) 624.
- 14 M. Genut, L. Margulis, G. Hodes and R. Tenne, *Thin Solid Films*, in the press.
- 15 J. C. Wildervanck and F. Jellink, *Z. Anorg. Allg. Chem.*, **328** (1964) 309.
- 16 S. P. Cramer, K. S. Liang, A. J. Jacobson, C. H. Chang and R. R. Chianelli, *Inorg. Chem.*, **23** (1984) 1215.
- 17 E. Y. Rode and B. A. Lebedev, *Zh. Neorg. Khim.*, **9** (1964) 2068.
- 18 M. Genut, L. Margulis, G. Hodes and R. Tenne, to be published.
- 19 A. Mallouk and J. C. Bernede, *Thin Solid Films*, **158** (1988) 285.